THE JOURNAL OF PHYSICAL CHEMISTRY B

Article

pubs.acs.org/JPCB

Small-Angle Neutron Scattering Study of Organic-Phase Aggregation in the TALSPEAK Process

Travis S. Grimes,[†,∥] Mark P. Jensen,[‡] Lisa Debeer-Schmidt,[§] Ken Littrell,[§] and Kenneth L. Nash*[,†]

[†]Chemistry Department, Washington State University, Pullman, Washington 99164, United States

[‡]Chemical Sciences and Engineering Division, Argonne National Laboratory, Argonne, Illinois 60439, United States

[§]High Flux Isotope Reactor, Oak Ridge National Laboratory, Oak Ridge, Tennessee 37831, United States

ABSTRACT: The Trivalent Actinide−Lanthanide Separation by Phosphorus reagent Extraction from Aqueous Komplexes (TALSPEAK) process is a solvent extraction based method for separating trivalent lanthanides (Ln^{3+}) from trivalent actinide cations in used nuclear fuel reprocessing. In conventional TALSPEAK, the extractant solution is di(2-ethylhexyl)phosphoric acid (HDEHP) in 1,4-diisopropylbenzene (DIPB). The aqueous medium is diethylenetriamine-*N*,*N*,*N*′,*N*″,*N*″-pentaacetic acid (DTPA) in a concentrated lactic acid (HL) buffer. Lanthanides are extracted by HDEHP/DIPB, while the actinides remain in the aqueous phase as DTPA complexes. Lactic acid is extracted both independently of the lanthanides and as Ln/HL/HDEHP mixed complex(es). Previous results indicate that lanthanides are extracted both as the mixed complex and as a binary $Ln(DEHP{\cdot}HDEHP)_3$ species. Small-angle neutron scattering (SANS) has been applied to study the self-organization properties of solute molecules in xylene solutions containing HDEHP, HL, selected lanthanide ions, and water. The scattering results demonstrate that the dominant HDEHP species is the hydrogen bonded dimer, $(HDEHP)_2$. Absent lanthanides, lactic acid is extracted as the 1:3 complex ($HL{\cdot}(HDEHP)_3$). Scattering in samples containing up to 0.005 M lanthanides (prepared by extracting lanthanides from aqueous media containing 1.0 M buffered lactic acid) indicates that the dominant metal complex is $Ln(DEHP{\cdot}HDEHP)_3$. At 0.013 M extracted lanthanide, the scattering results indicate lower Ln:DEHP stoichiometry and larger scattering particles. At higher metal concentrations, the SANS results indicate large aggregates, the largest aggregates achieving a size equivalent to 20 HDEHP monomers as the primary scattering entity. Analysis of particle shapes indicates best fits with a uniform oblate spheroid particle. These results are discussed in connection with the results of a number of complementary observations that have been made on this system.

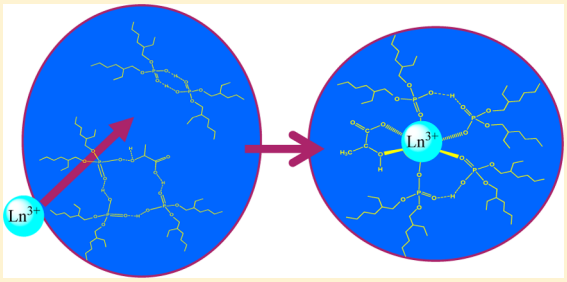

INTRODUCTION

A key component of nuclear fuel cycle science and technology is transmutation of the long-lived transplutonium actinides americium and curium. However, transmutation in nuclear reactors is possible only after these minor actinides (MAs) have been separated from the trivalent lanthanide fission products, several of which have high affinity for neutrons that are needed for actinide transmutation. Currently, the U.S. Department of Energy's Fuel Cycle Research and Development (FCR&D) program is considering the Trivalent Actinide−Lanthanide Separations by Phosphorus reagent Extraction from Aqueous Komplexes (TALSPEAK) process as a method to separate the trivalent lanthanide metals from the MAs in advanced nuclear fuel cycles. Recent research has focused on characterization of the fundamental chemistry of this solvent extraction system.[1−8]

TALSPEAK is a solvent extraction separation process that was developed for technological applications in the 1960s.[9,10] The process was designed to separate trivalent rare earth cations from the MAs (Am^{3+} and Cm^{3+}) to allow more efficient production of transplutonium actinides for scientific research. The trivalent 4f- and 5f-elements are hard acid cations,[11] thus they interact most strongly with hard base donors like F^- and O^{2-} and much less strongly with Cl^- and N donors. Because of the core-like nature of the 4f valence orbitals of lanthanides, the trivalent ions shrink in size by about 20% from La^{3+} to Lu^{3+}. As a result of this "lanthanide contraction", Ln^{3+} cations are similar in size to the isoelectronic actinide (An^{3+}) cations. The predominance of a single oxidation state and comparable size of the ions limits options for separating these two groups. TALSPEAK achieves the group separation by extraction of the trivalent rare earths using the dialkyl phosphorus extractant di(2-ethylhexyl)phosphoric acid (HDEHP or HA) from an aqueous medium containing the soft-donor complexing agent diethylenetriamine-*N*,*N*,*N*′,*N*″,*N*″-pentaacetic acid (DTPA), which selectively retains the trivalent MAs in the aqueous phase based on the slightly greater covalency of actinide bonding interactions.[12−14]

At low total metal concentrations and in most nonpolar diluents, the extraction of trivalent f-element cations by

Received: June 29, 2012
Revised: October 24, 2012
Published: October 29, 2012

HDEHP from mineral acid solutions proceeds according to the biphasic equilibrium expression,[15]

$$M^{3+} + 3(HDEHP)_{2(org)} \leftrightarrows M(DEHP{\cdot}HDEHP)_{3(org)} + 3H^{+} \quad (1)$$

where the organic phase species are designated by the subscript (org). If the extracted metal concentration exceeds the 1:6 metal/extractant ratio (considered to be the theoretical loading capacity) or if a polar (de-dimerizing) diluent is employed, the extraction also can proceed with HDEHP monomers with a 1:3 metal/extractant ratio.

$$M^{3+} + 3HDEHP_{(org)} \leftrightarrows M(DEHP)_{3(org)} + 3H^{+} \quad (2)$$

In the TALSPEAK process, DTPA preferentially complexes the trivalent actinides based on the general equilibrium expression

$$M^{3+} + H_nDTPA^{n-5} \leftrightarrows M(DTPA)^{2-} + nH^{+} \quad (3)$$

to keep them in the aqueous phase, enabling the group separation. Maintaining a constant pH is a fundamental requirement of the process, hence a buffer of suitable properties is also required.

To hold pH constant in the 2.5−4.0 range, the conventional TALSPEAK process employs a lactic acid buffer at high concentrations. Ultimately, 1.0−2.0 M HL became the preferred TALSPEAK aqueous medium/background electrolyte. During process development, it was observed that HL provided the best phase separation and increased the solubility of the aminopolycarboxylate complexants.[9,10] Investigations by Kolarik[16] indicated that high concentrations of HL improved phase-transfer kinetics in the system. This unconventional aqueous medium introduces several interesting complications into the chemistry that governs this system.

In prior investigations,[3,6] partitioning of HL and H_2O into TALSPEAK organic phases has been reported with two important results. First, during extraction, it was seen that HL partitions to the organic phase independent of the metal ion, in contrast to previous literature reports that generally linked lactate partitioning with lanthanide extraction.[9,10,17] Second, samples of 1.0 M HDEHP in 1,4-diisopropyl benzene (DIPB) contacted with 2.0 M lactic acid buffer were seen to contain more than 1.0 M dissolved H_2O and to have not achieved saturation with respect to lactic acid or water content.[3] Both high water miscibility and the apparent high lactic acid saturation limit (neither typically seen in solvent extraction reactions) raised questions concerning the organization of solute molecules in the extractant phase.

A subsequent report based on NMR/ESI−MS investigations of these systems gave a clear indication of the presence of mixed ligand complexes $(Ln(L)_n(DEHP)_{3-n})_2$ in the extractant phase under conditions of high lactate and lanthanide concentrations.[4] Both NMR and fluorescence spectroscopy have established that the conventional $Ln(DEHP{\cdot}HDEHP)_3$ complex is the dominant species at millimolar lanthanide concentrations, in both the presence and the absence of lactate.[4,6] At higher concentrations of lanthanide ions (extracted from lactate media), a different species is indicated by changes in the fluorescence emission of Eu^{3+}. ESI−MS results suggest that this species is most probably $Ln_2(L)_2(DEHP)_4$, likely featuring phosphate bridges between the lanthanide cations. NMR (^{31}P) spectroscopy establishes that (on the NMR time scale) this complex is substitution inert. The combination of a moderately acidic cation exchanging extractant with a highly charged cation of variable coordination geometry and an unconventional aqueous medium leads to an unusually complex solvent extraction system.

In the present investigation, small-angle neutron scattering (SANS) has been applied to examine the aggregation state of HDEHP in *p*-xylene-d_{10} after equilibration with aqueous phases containing varying amounts of lactic acid and lanthanide cations. In the HL−HDEHP series evidence is sought to determine whether or not HDEHP reorganizes under the influence of extracted lactic acid. In the Ln−HL−HDEHP series, information on the influence of lanthanide complexation on HDEHP organization is sought. In total, three sets of samples have been examined: (1) xylene solutions containing HDEHP alone, (2) xylene solutions containing a constant [HDEHP] equilibrated with aqueous media containing increasing amounts of lactate buffer at pH 3.6, and (3) xylene solutions prepared by HDEHP extraction of increasing concentrations of rare earth metal ions (La^{3+}, Gd^{3+}, Yb^{3+}) from 1.0 M lactate aqueous solutions. To complement the studies of HDEHP, samples prepared with a less acidic structural analog, 2-ethylhexyl phosphonic acid mono-2-ethylhexyl ester (HEH[EHP] or HB), were also examined.

EXPERIMENTAL METHODS

Materials. The HDEHP (97%) was purchased from Aldrich. The HEH[EHP] was graciously donated by EichromNPO Technologies. Both were purified by the copper precipitation method.[18] The purified HDEHP and the HEH[EHP] were determined to be 99.8% and 99.7% pure, respectively, by titration with NaOH. The organic diluents, *p*-xylene-d_{10} (99%, Sigma Aldrich) and 1,4-diisopropylbenzene (99%, Alfa Aesar), were used without further purification. The organic phase samples were prepared by dissolving weighed amounts of the purified HDEHP or HEH[EHP] in the appropriate diluent.

The aqueous phases were prepared from lanthanide nitrate stock solutions created from 99.999% lanthanide oxides or carbonates (Arris International Co.). The solutions were standardized to determine metal concentration, nitrate concentration, and H^+ concentration using ICP-MS and ion exchange chromatography (Dowex 50W-8X, H^+ form, 100−200 mesh) and potentiometric titrations. Lactic acid solutions were prepared fresh on the day of experimentation (from sodium lactate) to minimize the presence of acid-catalyzed condensation product polyesters, lactones, or lactides. Nitric acid was added to sodium lactate until the desired pH of 3.6 was reached. Sodium lactate was purchased as a 60% (w/w) aqueous solution from Alpha Aesar and standardized by titration after exchanging Na^+ for H^+ by cation exchange.

$NaNO_3$ (ACS Reagent grade) was purchased from GFS chemicals. The crystals were dissolved in deionized water, filtered through a fine glass frit filter, and recrystallized from hot water. The $NaNO_3$ solutions were then standardized using ion-exchange chromatography and potentiometric titrations. All aqueous solutions were prepared in 18 MΩ deionized water.

Sample Preparation. *HDEHP and HEH[EHP].* Samples of HDEHP and HEH[EHP] were prepared at 0.1 and 0.2 M by dissolving weighed amounts of extractant in *p*-xylene-d_{10}. The deuterated diluent is required in the SANS experiments to provide adequate contrast for the neutron scattering. SANS analysis was done on HDEHP samples before and after equilibration with aqueous lactate buffer media; separate series were prepared after equilibration with 0.1−2.0 M lactate and

dx.doi.org/10.1021/jp306451d | J. Phys. Chem. B 2012, 116, 13722−13730

Table 1. Organic Phase Samples Prepared for SANS Analysis

sample[a]	extractant	Ln^{3+}	[HA,HB][a], M	$[Ln^{3+}]_{org}$, M	$[HL]_{org}$, M	$[H_2O]_{org}$, M[b]	$[HA]/[Ln^{3+}]$	$[HL]/[Ln^{3+}]$	$[HA]_2/[HL]_{org}$
$HA_{0.1}$	HDEHP	–	0.1004	–	–	–	–	–	–
$HA_{0.2}$	HDEHP	–	0.2002	–	–	–	–	–	–
$HL_{0.1}$	HDEHP	–	0.2002	–	0.0005	0.043	–	–	200
$HL_{0.5}$	HDEHP	–	0.2002	–	0.0032	0.043	–	–	31.3
$HL_{1.0}$	HDEHP	–	0.2002	–	0.0095	0.060	–	–	10.5
$HL_{2.0}$	HDEHP	–	0.2002	–	0.0408	0.124	–	–	2.45
$HL_{1.0}$	HEH[EHP]	–	0.1992	–	0.0060	0.002	–	–	16.6
$La_{0.003}$	HDEHP	La^{3+}	0.1004	0.003	0.0048	–	33.5	1.6	10.4
$Yb_{0.005}$	HDEHP	Yb^{3+}	0.1004	0.005	0.0049	–	20.1	0.98	10.2
$Gd_{0.013}$	HDEHP	Gd^{3+}	0.1004	0.013	0.0127	–	7.7	0.98	3.95
$La_{0.023}$	HDEHP	La^{3+}	0.1004	0.023	0.0200	–	4.4	0.87	2.51
$La_{0.031}$	HDEHP	La^{3+}	0.1004	0.031	0.0265	–	3.2	0.85	1.9

[a]HA = HDEHP, HB = HEH[EHP]. [b]$[H_2O]_{org}$ for the Ln^{3+} metal systems was estimated to be 0.030 M for the scattering length density calculations.

after equilibration with 1.0 M lactate containing varying concentrations of lanthanide ions. Variable lactate samples were analyzed for lactate and water content and variable lanthanide samples for lanthanide and lactate content. HEH[EHP] samples were prepared and analyzed only after equilibration with 1.0 M lactate buffer.

Lactic Acid and Ln^{3+}. All samples were prepared using solvent extraction techniques. Equal volumes of organic phase and aqueous phase (0.5 mL) were contacted using vigorous shaking for 15 min followed by 15 min of centrifugation. Aqueous phase samples were pre-equilibrated with neat xylene, and organic phase samples were pre-equilibrated with 2.0 M $NaNO_3$.

The concentrations of HDEHP and HEH[EHP] for the lactic acid samples were 0.2 M. Aqueous phase lactic acid concentrations were varied from 0.1 to 2.0 M. The HDEHP concentration used for the Ln^{3+} metal samples was 0.1 M. Aqueous phase metal concentrations were: $[La^{3+}]$ (0.005, 0.025, and 0.035 M), $[Gd^{3+}]$ (0.015 M), and $[Yb^{3+}]$ (0.005 M). For the lanthanide-containing samples, aqueous phase lactate concentrations were held constant at 1.0 M. The aqueous phase acidity in all samples was adjusted to pH 3.6. Ionic strength was adjusted to 2.0 M using $NaNO_3$. Distribution ratios for metal ion extraction were determined by taking 100 μL samples of the aqueous phase before and after equilibration and diluting to 50 mL with 2% HNO_3 for analysis (of lanthanide content) by inductively coupled plasma mass spectrometry (Hewlett-Packard 4500 series).

Three series of samples were created for SANS analysis. The first series contained the HDEHP extractant at 0.1 and 0.2 M. These samples were dissolved in xylene with no further treatment before analysis and no aqueous contact. The second series contained 0.2 M extractant and different amounts of lactic acid partitioned from the aqueous phase. Series three samples contained 0.1 M extractant, equilibrium concentrations of lactic acid, and water from contact with a 1.0 M aqueous HL solution and the Ln^{3+} metal ions that were extracted from the aqueous phase. The compositions of all samples analyzed in this investigation are summarized in Table 1. The HDEHP samples that were prepared by dissolving weighed amounts into xylene without further treatment are designated by HA_x, where the subscript x represents the concentration of the HDEHP extractant (e.g., $HA_{0.1}$ represents HDEHP at 0.1 M). The second series of samples, in which 0.2 M HDEHP was contacted with aqueous media containing increasing amounts of HL, is designated by HL_x where the subscript x represents the aqueous phase HL concentration before equilibration (e.g., $HL_{0.1}$ represents 0.2 M HDEHP contacted with 0.1 M HL). In the third series of samples, 0.1 M HDEHP was contacted with different Ln^{3+} metal ions at varying concentrations in 1.0 M HL, and the samples are designated by Ln_x, where Ln is used to distinguish the lanthanide metal used and the x represents the organic phase concentration of the lanthanide metal (e.g., $La_{0.003}$ refers to the 0.003 M La^{3+} organic phase sample). These sample designators will be used to describe the samples throughout this report.

To establish the predominantly mononuclear nature of the extracted lanthanide complexes at $[Ln^{3+}]$ less than 0.005 M, extraction experiments were conducted (in triplicate) using the same procedures outlined in the previous section using aqueous media containing different concentrations of Eu^{3+}. Organic phase samples were prepared at 0.1 M HDEHP in 1,4-diisopropylbenzene. The total concentrations of Eu^{3+} were fixed for three experiments at 0.001, 0.0025, and 0.005 M. A 5 μL spike of ^{152,154}Eu was added to each aqueous phase sample after the pre-equilibration step to allow radiometric assay of both phases. The aqueous phase was 1.0 M HL, I = 2.0 M (NaL/$NaNO_3$), pH 3.6. After equilibration, a 300 μL sample was taken from each phase and analyzed by solid scintillation counting using a NaI(Tl) detector (Packard Cobra 5003) monitoring γ-radiation from ^{152,154}Eu.

SANS Measurements. SANS measurements were conducted at the Oak Ridge National Laboratory High Flux Isotope Reactor (HFIR) facility, on the general purpose (CG-2) SANS instrument.[19] The neutron wavelength, λ, was 4.75 Å ($\Delta\lambda/\lambda \sim 0.13$). The sample to detector distances used were 0.3, 4.0, and 18.5 m covering an overall range of scattering vectors (Q) from 0.003 to 0.947 Å^{-1}, where $Q = 4\pi\lambda^{-1} \sin\theta$ and 2θ is the scattering angle. The samples were contained in 12 mm diameter quartz cuvettes with a path length of 2 mm. SANS scattering profiles were collected at ambient temperature, approximately 23 ± 2 °C. Samples were corrected for background scattering using an empty cell and a deuterated solvent blank. Instrumental corrections and dark current corrections were also conducted. The scattering profiles were reduced to absolute scale using Igor Pro, and the data were analyzed using NIST Macros Version 3.[20]

RESULTS AND DISCUSSION

Small-Angle Neutron Scattering. Representative SANS scattering data for the full Q range collected are shown in Figure 1. SANS data are expressed as $I(Q)$ (intensity) vs Q

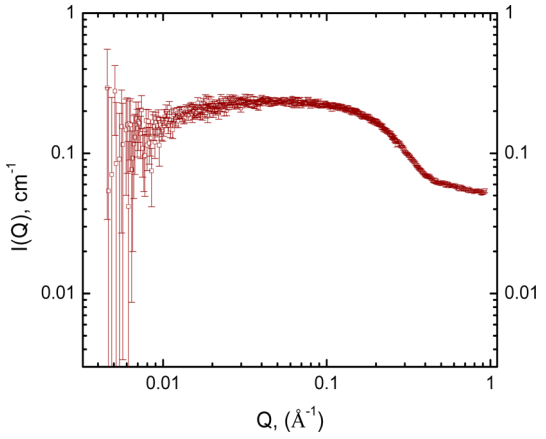

Figure 1. SANS scattering data of full Q range for $HA_{0.2}$ in *p*-xylene-d_{10} (0.2 M HDEHP).

(momentum transfer vector). The scattering intensity is proportional to the number of scattering nuclei in the sample and the respective characteristic scattering length of individual atoms. At high Q, scattering becomes more incoherent (as the scattering angle approaches 1 $Å^{-1}$ at which point it is no longer considered small-angle scattering). For analysis the data were truncated to a Q range of 0.03−0.4 $Å^{-1}$.

Guinier Analysis. Guinier analysis[21] is a useful technique to determine the radius of gyration (R_g) and the weight average aggregation number (n_w) from small-angle scattering data. The radius of gyration is a measure of the distribution of scattering centers as a function of their distance from the center of mass of the particle and is independent of the structure of the particle.[22,23] Scattering particle size can be estimated using the R_g to calculate volumes of the scattering particles employing a reasonable assumption about the particle shape.

Guinier analysis was performed on the scattering data; a sample from each series is shown in Figure 2. In a Guinier plot,[22] the scattering intensity at a given Q value is expressed as $\ln I(Q) = \ln I(0) - R_g^2/3Q^2$. The slope of this line is used to obtain R_g.

A restriction on the application of Guinier analysis is that it is only valid when $QR_g \leq 1$ (this is achieved by limiting the range of Q^2 values used for linear regression). The R_g is related to the physical radius of a corresponding uniform spherical particle, $R_{spherical}$, by the following equation.[24−27]

$$R_{spherical} = (5/3)^{1/2} R_g \tag{4}$$

The *y*-intercept of the Guinier analysis, ln $I(0)$, can be used to calculate the molecular weight of the HDEHP aggregates and from that value ultimately the aggregation number, as will be demonstrated. The scattering intensity is represented in eq 5[20,24,25]

$$I(Q) = N_p(\rho_p - \rho_s)^2 V_p^2 P(Q) S(Q) + I_{bkg} \tag{5}$$

where N_p is the number density of particles per unit volume; ρ_p and ρ_s are the scattering length densities of the extractant and the solvent, respectively; V_p is the volume of the scattering particles; $P(Q)$ is the particle form factor; $S(Q)$ is the structure factor;[22,23] and I_{bkg} represents the incoherent scattering background. In sufficiently dilute systems, in which interparticle interactions can be neglected, $S(Q) = 1$. At $Q = 0$, $P(Q) = 1$ and eq 5 can be expressed as[24−26,28−31]

$$I(0) = N_p(\rho_p - \rho_s)^2 V_p^2 \tag{6}$$

$I(0)$ is extracted directly from the *y*-intercept of the linear regression least-squares fit of the Guinier plot. Upon introduction of molar quantities and rearrangement of eq 6, the following equation, which allows estimation of n_w, the weight average aggregation number of HDEHP, is developed.[24−26,28−31]

$$n_w = \frac{M_W}{MW_{HA}} = \frac{6.022 \times 10^{26} \cdot d_{HA}^2 \cdot I(0)}{[HA]_{total} \cdot (\rho_p - \rho_S)^2 \cdot MW_{HA}^2} \tag{7}$$

In this equation, M_w represents the weight average molecular weight of HDEHP (or HEH[EHP]) in the aggregates; MW_{HA} is the molecular weight of HDEHP; d_{HA} is the density of the HDEHP (0.965 g/mL); and $[HA]_{total}$ is the total organic phase concentration of HDEHP. Inherent uncertainties in n_w arise from uncertainties in $I(0)$, d_{HA} (5%), and $[HA]_{total}$ (2%). The sum of uncertainties leads to 10−15% absolute uncertainty in the calculated aggregation number. An additional small systematic deviation in n_w (<5%) is introduced by not including scattering from organic phase HL or H_2O. The scattering length densities (ρ_p, ρ_s) of the extractant HDEHP and the diluent *p*-xylene-d_{10} are calculated by adding the individual scattering length densities of the individual atoms. The results of the Guinier analysis are summarized in Table 2.

0.2 M HDEHP and HEH[EHP] Equilibrated with Lactic Acid HL, ($HL_{0.1}$−$HL_{2.0}$, $HL_{1.0,HB}$). It is known from the results of earlier studies that both lactic acid and water are extracted by HDEHP into aromatic hydrocarbon solutions.[3,6] Water partitioning correlates in a complex fashion with the nature of the diluent, [HDEHP], and $[HL]_{org}$, though the previous results have not established the specific interactions that account for this partitioning. The results shown in Table 1 demonstrate that increasing concentrations of lactic acid are extracted into 0.2 M HDEHP as the samples are equilibrated with higher concentrations of lactate buffer. The sample contacted with 2.0 M lactate actually achieves a $[HL]_{org}$/[HDEHP] ratio of 0.2. If it is assumed that a constant HL:HDEHP stoichiometry defines the partitioning equilibrium for HL extraction and that all remaining HDEHP is present as the dimer, it should be possible to calculate an average HDEHP aggregation number based solely on knowledge of the

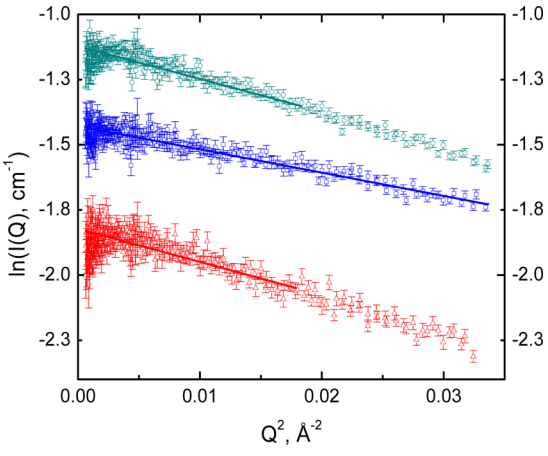

Figure 2. Guinier fit for (□) sample $HA_{0.2}$, 0.2 M HDEHP; (○) sample $HL_{2.0}$, 0.2 M HDEHP/0.0408 M lactic acid; and (Δ) sample $La_{0.003}$, 0.1 M HDEHP/0.003 M La^{3+}/0.0048 M lactic acid.

dx.doi.org/10.1021/jp306451d | J. Phys. Chem. B 2012, 116, 13722−13730

Table 2. Summary of Guinier Analysis, Radius of Gyration, Q Validation Range, and Weight Average Aggregation Number of HDEHP Extractant Samples in *p*-Xylene-d_{10}[a]

sample[b]	$I(0)$	R_g, Å	$Q_{max}{*}R_g$[c]	$R_{(spherical)}$, Å[d]	M_w, g/mol	n_w
$HA_{0.1}$	0.115 ± 0.001	5.20 ± 0.15	0.95	6.7 ± 0.5	620.4	1.92 ± 0.23
$HA_{0.2}$	0.240 ± 0.001	5.18 ± 0.09	0.95	6.7 ± 0.4	647.8	2.01 ± 0.23
$HL_{0.1}$	0.247 ± 0.002	5.28 ± 0.11	0.95	6.8 ± 0.1	647.1	2.01 ± 0.23
$HL_{0.5}$	0.253 ± 0.001	5.51 ± 0.10	0.97	7.1 ± 0.1	659.4	2.06 ± 0.24
$HL_{1.0}$	0.257 ± 0.002	5.38 ± 0.11	0.93	6.9 ± 0.1	668.6	2.08 ± 0.24
$HL_{2.0}$	0.326 ± 0.002	6.13 ± 0.14	0.93	7.9 ± 0.2	847.4	2.65 ± 0.31
$HL_{1.0,HB}$	0.222 ± 0.001	4.77 ± 0.10	0.96	6.2 ± 0.1	576.7	1.86 ± 0.22
$La_{0.003}$	0.162 ± 0.002	6.18 ± 0.19	0.94	8.0 ± 0.2	857.7	2.66 ± 0.32
$Yb_{0.005}$	0.164 ± 0.002	6.01 ± 0.20	0.94	7.8 ± 0.3	871	2.70 ± 0.33
$Gd_{0.013}$	0.213 ± 0.002	6.47 ± 0.17	1	8.3 ± 0.2	1130	3.50 ± 0.42
$La_{0.023}$	0.768 ± 0.006	12.89 ± 0.32	0.97	16.6 ± 0.4	4075.3	12.64 ± 1.50
$La_{0.031}$	0.971 ± 0.009	12.72 ± 0.41	0.91	16.4 ± 0.5	5152.3	15.98 ± 1.52

[a]All uncertainties are reported at the 95% confidence level. [b]HA = HDEHP, HB = HEH[EHP]. [c]Q_{max} is the maximum Q value used for linear regression in the Guinier analysis. [d]$R_{spherical}$ values calculated from R_g assuming spherical particles for HDEHP and HEH[EHP]aggregates.

concentrations of HDEHP and HL (Table 1). The appropriate expression for a calculated n_w^{calc} would be

$$n_w^{calc} = \frac{m^2\cdot[HL(HDEHP)_m] + 2^2\cdot[(HDEHP)_2]_{free}}{[HDEHP]_{tot}} \quad (8)$$

where $[(HDEHP)_2]_{free}$ represents all HDEHP not associated with lactic acid. HL does not partition into xylene independently of HDEHP, and monomeric HDEHP is a minor species in HDEHP solutions in nonpolar diluents. Knowing $[HL]_{org}$, a simple mass balance equation and insertion of the appropriate value for m should produce n_w^{calc} in agreement with the values calculated by Guinier analysis. Assuming m = 1, n_w^{calc} values decrease with HL extraction, ranging from 2.0 down to 1.8 as $[HL]_{org}$ increases; for m = 2, n_w^{calc} = 2.0 for all $[HL]_{org}$; for m = 3, the calculated values are $n_w^{calc}(HL_{0.1})$ = 2.01, $n_w^{calc}(HL_{0.5})$ = 2.05, $n_w^{calc}(HL_{1.0})$ = 2.14, and $n_w^{calc}(HL_{2.0})$ = 2.62, in general agreement with the scattering results shown in Table 2 (2.01, 2.06, 2.08, 2.65). These results are consistent with an earlier report in which $HL\cdot(HDEHP)_3$ was suggested as an important species based on the results of radiotracer distribution experiments.[6]

Sample $HL_{1.0,HB}$, 0.2 M HEH[EHP], contacted with 1.0 M lactic acid contained $[HL]_{org}$ = 0.006 M at equilibrium. The Guinier analysis for sample $HL_{1.0,HB}$ gives n_w = 1.86 ± 0.22, which is comparable to $HL_{1.0}$. Application of n_w^{calc} gives 2.09 if $HL\cdot(HEH[EHP])_3$ is assumed to be the extracted species, 1.97 if the 1:1 complex ($HL\cdot(HEH[EHP])$) is assumed. Though the 1:1 value appears more consistent with the scattering results, the experimental uncertainties are too large to decide between these options. However, it is noteworthy that in the HEH[EHP] system the scattering results do not give any indication of an $HL\cdot(HEH[EHP])_3$ species comparable to that seen in the HDEHP system.

Ln^{3+} Metal Ion Extraction into 0.1 M HDEHP ($La_{0.003}$–$La_{0.031}$, $Yb_{0.005}$, $Gd_{0.013}$). The results in Table 2 indicate that the aggregation number is more closely correlated with the organic phase concentration of the metal than the identity of the cation in this limited collection of five metal loaded samples. As noted above, the previously identified organic phase metal complexes in this system are $Ln(DEHP\cdot HDEHP)_3$ and $Ln_2(L)_2(DEHP)_4$. Eu^{3+} fluorescence and ESI–MS experiments have demonstrated that a shift from $Ln(DEHP\cdot HDEHP)_3$ to $Ln_2(L)_2(DEHP)_4$ occurs as the lanthanide concentration increases.

Lumetta and co-workers[32] have recently reported results from vapor pressure osmometry and radiometric slope analysis studies that have been interpreted to indicate that the predominant lanthanide complex in HDEHP solutions in *n*-dodecane is $Ln(DEHP\cdot HDEHP)_2(DEHP)$. The primary difference between that work and the present is the diluent, which likely accounts for this apparent difference in complex stoichiometry. In the interpretation of the present results, earlier NMR, ESI–MS, and lanthanide fluorescence results provide convincing evidence for the correctness of the $Ln(DEHP\cdot HDEHP)_3$ stoichiometry in the aromatic diluent used in the present work.

Assuming that these metal complexes, $(HDEHP)_2$, and $HL(HDEHP)_3$ represent the most important species to account for the observed scattering, the following mass balance expressions can be used to correlate known species with the observed neutron scattering results.

$$[Ln]_{t\,org} = [Ln(DEHP\cdot HDEHP)_3] + 2\cdot[Ln_2(L)_2(DEHP)_4] \quad (9)$$

$$[HL]_{t\,org} = [HL(HDEHP)_3] + 2\cdot[Ln_2(L)_2(DEHP)_4] \quad (10)$$

$$[HDEHP]_{t\,org} = 2\cdot[(HDEHP)_2] + 3\cdot[HL(HDEHP)_3] + 6\cdot[Ln(DEHP\cdot HDEHP)_3] + 4\cdot[Ln_2(L)_2(DEHP)_4] \quad (11)$$

HDEHP represents the primary source of neutron scattering in these samples. Neither the metal ion nor the lactate contribute significantly to particle contrast in these complexes.

Taking these relationships and species into account, the modified expression for a calculated n_w^{calc} when lanthanides are present would be:

$$n_w^{calc} = \{6^2\cdot[Ln(DEHP\cdot HDEHP)_3] + 2^2\cdot[(HDEHP)_2]_{free} + 3^2\cdot[HL(HDEHP)_3] + 4^2\cdot[Ln_2L_2(DEHP)_4]\} / [HDEHP]_{tot} \quad (12)$$

In sample $La_{0.003}$, Guinier analysis indicates n_w = 2.66 ± 0.32 for a sample containing 0.003 M La^{3+}, 0.0048 M HL, and 0.1004 M HDEHP. The earlier fluorescence results suggest that $La(DEHP\cdot HDEHP)_3$ should be the dominant metal complex in

dx.doi.org/10.1021/jp306451d | J. Phys. Chem. B 2012, 116, 13722–13730

Table 3. Nonlinear Least-Squares Analysis for the Noninteracting Uniform Ellipsoid Form Factor[a]

sample	volume fraction	$(\rho_p - \rho_s)^2$, $(10^{21}$ cm$^{-4})^b$	R_a, Å	R_b, Å	I_{bkg}, (cm$^{-1})^c$	reduced χ^2	ellipsoid vol. (Å^3)	experimental n_w
$HA_{0.2}$	0.0669	3.22	2.79 ± 0.08	9.14 ± 0.12	0.032	1.5	976 ± 33	1.76 ± 0.06
$HL_{0.1}$	0.0677	3.34	2.72 ± 0.08	9.30 ± 0.12	0.030	2	985 ± 34	1.76 ± 0.06
$HL_{0.5}$	0.0679	3.32	2.65 ± 0.06	9.54 ± 0.10	0.028	1.7	1010 ± 27	1.79 ± 0.05
$HL_{1.0}$	0.0687	3.33	2.63 ± 0.06	9.66 ± 0.10	0.027	2	1028 ± 28	1.80 ± 0.05
$HL_{2.0}$	0.0722	3.32	2.47 ± 0.02	11.07 ± 0.08	0.029	2.4	1268 ± 24	2.12 ± 0.04
$HL_{1.0,HB}$	0.0638	3.21	3.40 ± 0.16	8.22 ± 0.16	0.027	1.8	962 ± 52	1.82 ± 0.10
$La_{0.003}$	0.0344	3.26	2.65 ± 0.06	11.08 ± 0.12	0.013	1.6	1363 ± 37	2.39 ± 0.07
$Yb_{0.005}$	0.0344	3.22	2.89 ± 0.04	10.69 ± 0.12	0.014	1.8	1383 ± 44	2.43 ± 0.08
$Gd_{0.013}$	0.0351	3.01	4.15 ± 0.06	11.01 ± 0.10	0.014	3.4	2107 ± 41	3.63 ± 0.07
$La_{0.023}$	0.0354	2.79	4.19 ± 0.02	21.75 ± 0.06	0.120	2.9	8303 ± 51	14.17 ± 0.09
$La_{0.031}$	0.0358	2.68	5.52 ± 0.02	22.31 ± 0.06	0.001	9.1	11509 ± 60	19.45 ± 0.10

[a] R_a represents the minor axis (the rotation axis) and R_b represents the major axis. [HDEHP] = 0.2 M in samples, $HA_{0.2}$, $HL_{0.1}$–$HL_{2.0}$, and $HL_{1.0,HB}$ and 0.1 M in samples $La_{0.003}$–$La_{0.031}$, $Yb_{0.005}$, and $Gd_{0.013}$. All uncertainties are reported at the 95% confidence level. [b] $\rho_s = 5.74 \times 10^{10}$ cm^{-2}. [c] Uncertainties associated with I_{bkg}: ±0.002.

this lanthanide concentration range, and thus the computation started with the assumption that all of the La^{3+} is present as $La(DEHP{\cdot}HDEHP)_3$ and all of the HL_{org} is $HL(HDEHP)_3$. With this assumption, n_w^{calc} is 2.86. Successive apportioning of La^{3+} to the species $La_2L_2(DEHP)_4$, and adjustment of [HL] and [HDEHP] to compensate for this adjustment using eqs 9–11, indicates that n_w^{calc} = 2.66 is seen at 70% $La(DEHP{\cdot}HDEHP)_3$/30% $La_2L_2(DEHP)_4$.

Lending additional support to the predominance of the mononuclear metal complex under these conditions, the Eu^{3+} extraction data at variable total Eu^{3+}/1.0 M HL/0.1 M HDEHP give the following results: $[Eu^{3+}]_t$ = 0.001 M, D_{Eu} = 0.202 ± 0.002; $[Eu^{3+}]_t$ = 0.0025 M, D_{Eu} = 0.201 ± 0.004; $[Eu^{3+}]_t$ = 0.005 M, D_{Eu} = 0.194 ± 0.005. The constant D values establish the independence of extraction equilibria from changes in $[Eu^{3+}]$, confirming the dominance of the mononuclear complex.

In samples $Yb_{0.005}$ (n_w = 2.70 ± 0.33) and $Gd_{0.013}$ (n_w = 3.50 ± 0.42), the earlier fluorescence results indicate the presence of both $Ln(DEHP{\cdot}HDEHP)_3$ and $Ln(L)_2(DEHP)_4$, with the latter becoming increasingly important as the lanthanide concentration increases.[6] Following the same procedure as described above, the n_w value for sample $Yb_{0.005}$ was best replicated by assuming Yb^{3+} was partitioned 45% to $[Yb(DEHP{\cdot}HDEHP)_3]$ (= 0.00225 M), 55% to $Yb_2(L)_2(DEHP)_4$ (= 0.00137 M), $[HL(HDEHP)_3]$ = 0.00215 M, and $[(HDEHP)_2]$ = 0.0373 M. For sample $Gd_{0.013}$, the n_w value is reproduced by partitioning Gd^{3+} 33% to $[Gd(DEHP{\cdot}HDEHP)_3]$ (= 0.00429 M) and 67% to $Gd_2(L)_2(DEHP)_4$ (= 0.00436 M), leaving $[HL(HDEHP)_3]$ = 0.00399 M, $[(HDEHP)_2]$ = 0.0224 M.

The R_g values for samples $La_{0.003}$ and $Yb_{0.005}$ are in agreement within experimental error, suggesting similar size and shape of the average scattering particle. On the basis of the above analysis, 75% of the scattering particles are $(HDEHP)_2$ in each of these samples. This implies similar structures for the Ln^{3+}/HDEHP complexes at low metal-loading conditions, and extraction likely proceeds predominantly as described in eq 1 when the metal ion concentration remains well below the theoretical loading capacity (or the 1:6 metal ligand ratio). The data show an increase in the particle volume for the $Gd_{0.013}$ sample. The n_w^{calc} values indicate that the distribution of HDEHP among the projected species is 45% $(HDEHP)_2$, 26% $Gd(DEHP{\cdot}HDEHP)_3$, 17% $Gd_2(L)_2(DEHP)_4$, and 12% $HL(HDEHP)_3$.

As the extracted metal ion concentration continues to increase ($La_{0.023}$ and $La_{0.031}$), the measured aggregation numbers increase dramatically. In this concentration limit, the $[HDEHP]/[Ln]_{org}$ ratio drops to 4.4 and then to 3.2. On the basis of the trend seen in the $La_{0.003}$, $Yb_{0.005}$, and $Gd_{0.013}$ samples, it is reasonable to assume that species of the general form $(Ln_2(L)_2(DEHP)_4)_n$ represent an increasing fraction of all neutron scatterers in the $La_{0.023}$ and $La_{0.031}$ samples. It is not possible to project from these results whether the larger aggregates represent phosphate-bridged polylanthanide chains or aggregates of discrete $Ln_2(L)_{2+x}(DEHP)_{4-x}$ complexes.

Nonlinear Least-Squares Analysis. To complement the Guinier analysis (which is independent of particle shape), a more detailed analysis of the average particle shape can be conducted by fitting particle form factors (eq 5) to the scattering data.[20] This approach allows for a more accurate calculation of experimental parameters and consideration of the influence of HL and H_2O on n_w. While fitting eq 5 to the experimental data, contrast factors ($(\rho_p - \rho_s)^2$, calculated for each sample using scattering length densities) and volume fractions ($N_p{\cdot}V_p$, calculated directly from the concentrations of the solutes for each sample, e.g., HDEHP or HEH[EHP], lactic acid, and H_2O) were held constant. Geometric parameters (such as radii) specific to individual form factors (e.g., sphere, cylinder, uniform ellipsoid) were varied in the fitting, as was I_{bkg}. The particle volumes were calculated from the geometric parameters, and n_w was determined from the particle volumes (Table 3) as previously described.[26] The results of these fitting exercises are shown in Figure 3. The changing shape of the scattering curve for $HL_{2.0}$ is an indication of a shift away from $(HDEHP)_2$ as the primary scattering species to some $HL{\cdot}(HDEHP)_n$ species. The noninteracting uniform ellipsoid[20] was found to best fit the scattering results for all three series of samples (Table 3). All HDEHP samples are best fit with species having a disk-like morphology in this medium.

0.2 M HDEHP Equilibrated with 0.1–2.0 M HL ($HL_{0.1}$–$HL_{2.0}$, $HL_{1.0,HB}$). In the series HA, $HL_{0.1}$–$HL_{2.0}$, the particle volume increases steadily with increasing [HL]. The scattering particle for the $HL_{1.0,HB}$ sample (HEH[EHP] equilibrated with 1.0 M sodium lactate buffer) has a volume nearly identical with that of sample $HA_{0.2}$ (0.2 M HDEHP), though the aspect ratio of the disk is reduced (r_b/r_a = 2.4 vs 3.3 for the HDEHP dimer). It is known from previous work[5] that HEH[EHP] has a much lower tendency to extract HL than HDEHP, and hence the size and shape of the scattering particle is less impacted by

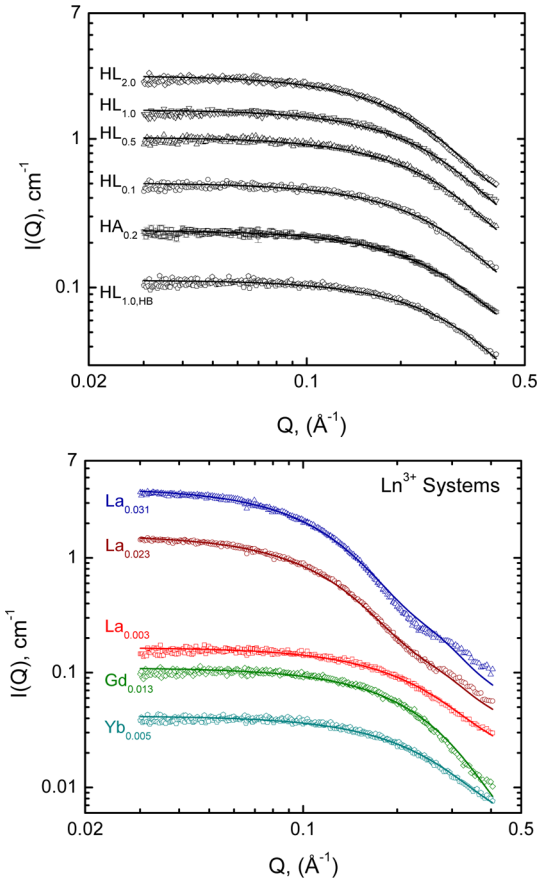

Figure 3. Nonlinear least-squares fitting results for samples $HA_{0.2}$, $HL_{0.1}$–$HL_{2.0}$, $HL_{1.0,HB}$, nonmetal systems, and samples $La_{0.001}$–$La_{0.031}$, $Gd_{0.013}$, and $Yb_{0.005}$. Samples $HA_{0.2}$ and $La_{0.003}$ are reported at the correct intensity, and the uncertainties used to weight the fits are shown in $HA_{0.2}$. Data sets for samples $HL_{0.1}$–$HL_{2.0}$ and $La_{0.023}$ and $La_{0.031}$ are offset vertically by increasing factors of 2. The data sets for samples $HL_{1.0,HB}$, $Gd_{0.013}$, and $Yb_{0.005}$ are shifted downward by increasing factors of 2. Uncertainties in the data points are omitted for clarity of the continuous fit line and are similar to the error shown for sample $HA_{0.2}$.

extraction of HL, even after contact with 1.0 M HL/NaL. The volume of the average scattering particle for samples $HL_{0.1}$ to $HL_{2.0}$ increases steadily as $[HL]_{org}$ increases. For sample $HL_{2.0}$, in which $[HL]_{org}$ reaches 0.040 M ($[HDEHP]/[HL] = 5$), the volume of the scattering particle increases 20% from sample $HL_{1.0}$. The average particle in this sample is significantly wider and slightly flattened ($r_b/r_a = 4.7$), perhaps indicating that a species $HL{\cdot}(HDEHP)_3$ has become the dominant scattering particle under these conditions, as has been noted above.

Figure 4 demonstrates a linear relationship between the aspect ratio and aqueous phase lactate concentration for the HDEHP-HL samples. This result implies a direct interaction between HL and HDEHP, possibly forming a cyclic ring structure that includes one HL molecule and up to three HDEHP monomers. Such a complex could account for both the observed stoichiometry and the elongated particles. Proper orientation of the carboxylate and the hydroxyl groups would provide the necessary hydrogen bonding sites to form such a species. This cyclic ring structure would widen the original pocket created by the HDEHP dimer, perhaps contributing to the changing stoichiometry of the extracted lanthanide complexes at high lanthanide concentrations. The relationship

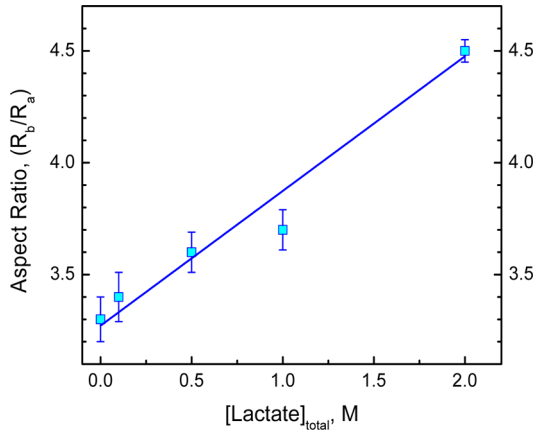

Figure 4. Linear dependence of the aspect ratio of the scattering particles for samples $HL_{0.1}$–$HL_{2.0}$ on aqueous phase lactate concentrations.

between the $HL{\cdot}(HDEHP)_n$ species and extracted lanthanide–lactate complexes has not been established, though the mixed ligand complexes have been seen.

It is known from earlier results that significant amounts of water are also extracted into the extractant phase in the company of HL. Due to the small molar volume of H_2O (relative to xylene, HDEHP, and lactate), water is believed to have only a small influence on the shape and size of these particles. The SANS experiment does not reveal the location of water molecules. A scattering experiment employing only D_2O as a contrast agent provided results that were difficult to interpret.

Finally, it is noteworthy that samples $HL_{1.0,HB}$ (0.2 M HEH[EHP], $[HL]_{aq}$ = 1.0 M) and HA (0.2 M HDEHP) present scattering particles with constant ellipsoid volumes but different shapes for those particles. The HEH[EHP] particle morphology is not as flat as the HDEHP scattering particles, though each extractant is certainly dimerized in xylene. The only difference between the extractants is the removal of one phosphate oxygen atom from HDEHP to "create" HEH[EHP]. Loss of an O atom in the structure slightly increases the basicity of the HO_2P– polar head of the extractant molecule, which lowers the dimerization constant but should have minimal impact on the structure of the dimerized extractant. The altered aspect ratio of the HEH[EHP] scattering particle suggests that the removal of this O atom causes one of the two 2-ethylhexyl groups to be directed more out of the plane that defines the basic structure of the disk-like scattering particle. A simple molecular modeling exercise has established this essential feature of the two extractant molecules.

Ln^{3+} Metal Ion Extraction with 0.1 M HDEHP ($La_{0.003}$–$La_{0.031}$, $Gd_{0.013}$, $Yb_{0.005}$). For samples $La_{0.003}$ and $Yb_{0.005}$, the average size and shape of the scattering particles are about 35% larger than the analogous HDEHP sample equilibrated with lactate alone ($HL_{1.0}$), though only 10% larger than the $HL_{2.0}$ sample. From the results of the Guinier analysis above, it is likely that the scattering results from the average effect of scattering from $Ln(DEHP{\cdot}HDEHP)_3$ and $(HDEHP)_2$ particles, with some contribution from $HL{\cdot}(HDEHP)_n$ species. In $La_{0.003}$ about 14% of the HDEHP is complexed to the metal ion (86% as $(HDEHP)_2$ + $HL{\cdot}(HDEHP)_n$), and in $Yb_{0.005}$ the corresponding ratios are 19%:81%. For $Gd_{0.013}$, the Guinier analysis, earlier ESI–MS/NMR,[4] and fluorescence spectroscopy[6] results indicate that the metal ion is present as a mixture of

dx.doi.org/10.1021/jp306451d | J. Phys. Chem. B 2012, 116, 13722–13730

$Gd(DEHP{\cdot}HDEHP)_3$ and $Gd_2(L)_2(DEHP)_4$. On the basis of n_w^{calc} analysis, the ratio of cation-bound to free/lactic acid associated HDEHP is approximately 68%:32%. In this sample, the ellipsoid volume is double that of the HDEHP dimer, though the aspect ratio is 1/3 smaller; e.g., the average scattering particle is 15% longer but nearly 60% thicker.

On the basis of the quality of the nonlinear fits as judged visually and by the reduced χ^2 values, it is apparent at the highest metal loading with La^{3+} ($La_{0.023}$ and $La_{0.031}$) that the uniform ellipsoid form factor is a less satisfactory model for the particle shapes. The inability of the uniform ellipsoid to model the particle shape may indicate increased polydispersity in the organic phase under these conditions or longer-scale organization of the scattering particles. Results of parallel studies using ^{31}P NMR suggest the presence of at least three different phosphorus environments under high metal loading conditions ($[La^{3+}]_{org}$ > 0.010 M).[4] ESI−MS results obtained under the same extraction conditions (0.1 M HDEHP, 0.5 M HL, pH 3.6) indicate that when $[La^{3+}]_{org}$ is 0.052 M, Ln^{3+}/HDEHP complexes appear to self-assemble into polynuclear species $(Ln{:}L{:}DEHP_2)_2$ in the organic phase.[4] It is possible in the highest lanthanide loading samples that there exists a mixture of the expected extracted complexes and polynuclear complexes, thus preventing the fitting of the scattering data using only one form factor. For the purposes of this analysis, it is assumed at these Ln^{3+} concentrations (0.023 and 0.031 M) that polynuclear complexes and/or oligomers are the dominant species in the organic phase.

CONCLUSIONS

In this study the organization of solute species in organic solutions relevant to the TALSPEAK process for trivalent actinide/lanthanide separations has been investigated using small-angle neutron scattering (SANS). This study continues complementary examinations of the same system using lanthanide fluorescence,[6] UV−visible spectrophotometry,[2] NMR spectroscopy/ESI−MS,[4] and radiotracer distribution studies.[3] The results of the SANS experiments establish that the predominant form of the HDEHP extractant in xylene is the hydrogen-bonded dimer. As lactic acid extraction increases, larger aggregates are seen, indicating association between extracted lactate and HDEHP. Consistent with an earlier report, the structurally analogous dialkyl phosphonic acid extractant HEH[EHP] interacts less strongly with lactic acid, and the dimer remains the predominant species.

As lanthanide metal ions are introduced (La^{3+}, Gd^{3+}, and Yb^{3+}), the scattering data indicate the presence of particles of larger dimensions. Modeling of scattering data indicates that the conventional lanthanide complex $Ln(DEHP{\cdot}HDEHP)_3$ is the predominant species up to about 0.005 M total extracted lanthanide with complementary (and independent) extraction of HL by HDEHP. This result matches the predictions of Eu^{3+} fluorescence studies, which also indicate a change in lanthanide speciation above 0.005 M. The appearance of larger species in the 0.013 M Gd^{3+} sample is reasonably consistent with a model that predicts a predominant $Ln_2(L)_2(DEHP)_4$ species that was seen in the earlier ESI−MS and NMR investigation. A shift toward much larger aggregates and a more complex mix of sizes of scattering particles are indicated at lanthanide concentrations above 0.02 M (in 0.1 M HDEHP). In this limit much larger aggregates representing 14 to 20 monomer HDEHP units are seen to dominate neutron scattering. It is not clear from these data whether these large scattering particles represent polynuclear complexes as proposed in the NMR/ESI−MS study or aggregates of smaller coordination complexes assembled through hydrophobic interactions. As each of the solutions investigated demonstrated no precipitation up to the stated metal loading, these species appear to possess a degree of stability as solution-phase species.

Finally, the application of nonlinear least-squares analytical methods of analysis to allow insights into the shape of the particles indicates that the predominant form for the scattering particles is noninteracting uniform ellipsoid of varying dimensions. An unexpected result from this portion of the investigation was the observation of slightly more rounded spheroids for the phosphonic acid dimer than is seen for the phosphoric acid extractant. Whether this difference in morphology is responsible for the greatly reduced tendency of the HEH[EHP] extractant to aid partitioning of lactic acid into the organic phase than is seen for HDEHP is an interesting possibility to consider. Solutions dominated by higher concentrations of lanthanide−HDEHP also produced oblate spheroid scattering particles, though of larger dimensions than the metal-free systems.

AUTHOR INFORMATION

Corresponding Author

*Phone: 509-335-2654. Fax: 509-335-8867. E-mail: knash@wsu.edu.

Present Address

[‖]Aqueous Separations and Radiochemistry Department, Idaho National Laboratory, Idaho Falls, Idaho 83401, United States.

Notes

The authors declare no competing financial interest.

ACKNOWLEDGMENTS

This work was supported by the U.S. Department of Energy Office of Nuclear Energy Science and Technology under the Nuclear Energy Research Initiative-Consortium (NERI-C) program under project number DE-FC07-02ID14896. Work by MPJ was supported by the U.S. Department of Energy, Assistant Secretary of the Office of Nuclear Energy, Advanced Fuel Cycle Initiative, under contract number DE-AC02-06CH11357 to UChicago Argonne LLC, operator of Argonne National Laboratory.

Use of this Research at Oak Ridge National Laboratory's High Flux Isotope Reactor was sponsored by the Scientific User Facilities Division, Office of Basic Energy Sciences, U.S. Department of Energy.

Dr. Mark Antonio is acknowledged for assistance in data analysis, guidance, and insightful discussions regarding experimental results.

REFERENCES

(1) Nilsson, M.; Nash, K. L. *Solvent Extr. Ion Exch.* **2009**, *237*, 354−377.

(2) Leggett, C. J.; Liu, G. K.; Jensen, M. P. *Solvent Extr. Ion Exch.* **2010**, *28*, 313−333.

(3) Grimes, T. S.; Nilsson, M. A.; Nash, K. L. *Sep. Sci. Technol.* **2010**, *45*, 1725−1732.

(4) Marie, C; Hiscox, B; Nash, K. L. *Dalton Trans.* **2012**, *4* (1), 1054.

(5) Braley, J. C.; Grimes, T. S.; Nash, K. L. *Ind. Eng. Chem. Res.* **2012**, *51*, 629−638.

(6) Grimes, T. S.; Tian, G.; Rao, L.; Nash, K. L. *Inorg. Chem.* **2012**, *51*, 6299−6307.

(7) Tian, G.; Martin, L. R.; Rao, L. *Inorg. Chem.* **2010**, *49*, 10598−10605.
(8) Tian, G.; Rao, L. *Sep. Sci. Technol.* **2010**, *45*, 1718−1724.
(9) Weaver, B.; Kappelman, F. A. *TALSPEAK, A New Method of Separating Americium and Curium from the Lanthanides by Extraction from Aqueous Solution of an Aminopolyacetic Acid Complex with a Monoacetic Organophosphate or Phosphonate*; Report ORNL-3559; Oak Ridge National Laboratory: Oakridge, TN, August 1964.
(10) Weaver, B.; Kapplemann, F. A. *J. Inorg. Nucl. Chem.* **1960**, *30*, 263−272.
(11) Aspinall, H. *Chemistry of the f-Block Elements*, 5th ed.; Gordon & Breach: Australia, 2001.
(12) Jensen, M. P.; Bond, A. H. *J. Am. Chem. Soc.* **2002**, *124*, 9870−9877.
(13) Choppin, G. R.; Nash, K. L. *Radiochim. Acta* **1995**, *70/71*, 225−236.
(14) Kozimor, S. A.; Yang, P.; Batista, E. R.; Boland, K. S.; Burns, C. J.; Clark, D. L.; Conradson, S. D.; Martin Wilkerson, M. P.; Wolfsberg, L. E. *J. Am. Chem. Soc.* **2009**, *131*, 12125−12136.
(15) Peppard, D. F.; Mason, G. W.; Driscoll, W. J.; Sironen, R. J. *J. Inorg. Nucl. Chem.* **1958**, *7*, 276−285.
(16) Kolařík, Z.; Kuhn, W. Acid organophosphorus-XXI. Kinetics and equilibriums of extraction of Eu(III) by di(2-ethylhexyl) phosphoric acid from complexing media. *Proceedings of International Solvent Extraction Conference*, London, England, 1974.
(17) Kosyakov, N. V.; Yerin, E. A. *J. Radioanal. Chem.* **1980**, *56*, 93−104.
(18) Partridge, J. A.; Jensen, R. C. *J. Inorg. Nucl. Chem.* **1969**, *31*, 2587−2589.
(19) General-Purpose Small-Angle Neutron Scattering Diffractometer Instrument Specifications Page. http://neutrons.ornl.gov/instruments/HFIR/CG2/ (accessed Mar 2012).
(20) Kline, S. R. *J. Appl. Crystallogr.* **2006**, *39*, 895.
(21) Guinier, A.; Fournet, G.; Walker, C. B.; Yudowitch, K. L. Chapter 2, General theory; Chapter 4, Methods of interpretation of experimental results. *Small-Angle Scattering of X-Rays*; John Wiley and Sons, Inc.: New York, NY, 1955; *5*−*78*, pp 126−160.
(22) Feigin, L. A.; Svergun, D. I. Determination of the integral parameters of particles. In *Structure Analysis by Small-Angle X-ray and Neutron Scattering*; Taylor, G. W., Ed.; Plenum Press, New York, NY, 1987; pp 59−105.
(23) Chiarizia, R.; Urban, V.; Thiyagarajan, P.; Herlinger, A. W. *Solvent Extr. Ion Exch.* **1998**, *16*, 1257−1278.
(24) Jensen, M. P.; Chiarizia, R.; Urban, V. *Solvent Extr. Ion Exch.* **2001**, *19*, 865−884.
(25) Yaita, T.; Herlinger, A. W.; Thiyagarajan, P.; Jensen, M. P. *Solvent Extr. Ion Exch.* **2004**, *22*, 553−571.
(26) Pedersen, J. S. *Adv. Colloid Interface Sci.* **1977**, *70*, 171−210.
(27) Chiarizia, R.; Urban, V.; Thiyagarajan, P.; Herlinger, A. W. *Solvent Extr. Ion Exch.* **1999**, *17*, 1171−1194.
(28) Chiarizia, R.; Urban, V.; Thiyagarajan, P.; Herlinger, A. W. *Solvent Extr. Ion Exch.* **1999**, *17*, 113−132.
(29) Chiarizia, R.; Jensen, M. P.; Rickert, P. G.; Kolarik, Z.; Borkowski, M.; Thiyagarajan, P. *Langmuir* **2004**, *20*, 10798−10808.
(30) Jensen, M. P.; Yaita, T.; Chiarizia, R. *Langmuir* **2007**, *23*, 4765−4774.
(31) Miralles, N.; Sastre, A.; Martinez, M.; Aguilar, M. *Anal. Sci.* **1992**, *8*, 773−777.
(32) Lumetta, G. J.; Levitskaya, T. G.; Latesky, S. L.; Henderson, R. V.; Edwards, E. A.; Braley, J. C.; Sinkov, S. I. *J. Coord. Chem.* **2012**, *65*, 741−753.